# Remediation of 2,4,6-Trichlorophenol from Aqueous Solution by Raw and Chemical Modified Date Palm Stone Biomass: Kinetics and Isotherms Studies

Nadavala Siva Kumar,[a,*] Mohammad Asif,[a] Anesh Manjaly Poulose,[b] Ebrahim H. Al-Ghurabi,[a] Shaddad S. Alhamedi,[a] and Janardhan Reddy Koduru [c]

Raw and citric acid chemically treated date palm stone agro-waste biomass (RDSB and CA-MDSB) powders were used to remove an important class of emerging industrial pollutants, *i.e.*, 2,4,6-trichlorophenol (2,4,6-TCP) from aqueous solutions towards sustainable waste utilization to develop cost-effective technology for treating wastewater. The biomass characterization was performed by using different analytical techniques such as CHN elemental analysis, particle size, BET, FTIR, and SEM-EDX, TGA analysis. The FTIR spectral analysis revealed that the main chemical groups (N–C, O=C, H-O, H-C, and O–C) were involved in trapping 2,4,6-TCP. The highest adsorption was achieved with a contact time of 150 and 120 min, an initial concentration of 50-200 mg/L, and a biosorbent dosage ranging from 0.1 to 1.0 g/L RDSB and CA-MDSB, respectively. The experimental kinetic data of the adsorption process for both adsorbents (RDSB and CA-MDSB) fitted very well with the pseudo-second-order kinetic model and Langmuir equilibrium data. The 2,4,6-TCP maximum monolayer adsorption capacities were 53.7, and 123.8 mg/g for RDSB and CA-MDSB, respectively. The present research confirms that the date palm stone biomass could be used as an effective and low-cost biosorbent for the remediation of 2,4,6-TCP from an aqueous environment.

*DOI: 10.15376/biores.19.2.3543-3570*

*Keywords: Adsorption; Date palm stone; Characterization; 2,4,6-trichlorophenol; Kinetics and Isotherm modeling*

*Contact information: a: Department of Chemical Engineering, College of Engineering, King Saud University, P.O. Box 800, Riyadh 11421, Saudi Arabia; b: Department of Chemical Engineering, SABIC Polymer Research Centre, King Saud University, P.O. Box 800, Riyadh 11421, Saudi Arabia; c: Department of Environmental Engineering, Kwangwoon University, Seoul 01897, Republic of Korea; *Corresponding author: snadavala@ksu.edu.sa*

## INTRODUCTION

Industries have a significant impact on our natural environment, especially aquatic ecosystems. Chemicals used in the manufacturing process, such as petrochemicals, paints, plastics, pharmaceuticals, oils, detergents, pesticides, herbicides, and paper-making release industrial organic effluents that contain phenol and chlorophenol derivatives (Priyanka *et al.* 2014; Soltani Goharrizi *et al.* 2019; Nazal *et al.* 2021). These chemicals are hazardous to human health and the environment. 2,4,6-Trichlorophenol (2,4,6-TCP) is particularly dangerous due to its special chemical structure, high level of toxicity, strong odor emission, persistence in the environment, and carcinogenic properties. The United States Environmental Protection Agency has listed most phenolic pollutants as a potential threat to living organisms (US EPA 1977). Therefore, it is crucial to remove these pollutants from

contaminated sites and treat wastewater before discharging it into the water circulatory system.

Several techniques have been employed to eradicate phenolic derivative compounds from wastewater, including biodegradation, chemical, biological, electrochemical, photochemical, and catalytic processes (Baker *et al.* 1980; Ahmaruzzaman 2008; Wang *et al.* 2012; Villegas *et al.* 2016; Nazal *et al.* 2021; Zada *et al.* 2021; Grace Pavithra *et al.* 2023). However, some of these techniques are costly and have high energy consumption due to the complexity of treatment processes and the production of toxic by-products or specific conditions. The adsorption technique has become a popular option due to its ease of operation, cost-effectiveness, environmental compatibility, flexibility, lack of secondary pollution, and efficient performance in treating phenolic wastewater (Crini *et al.* 2019; Ho 2022; Abdulrahman *et al.* 2023; Hyder *et al.* 2023). As a result, many researchers are selecting suitable adsorbents from industrial and agricultural waste products for the remediation of phenolic pollutants (Kurnik *et al.* 2015; Dehghani *et al.* 2023). Agro-waste biomass adsorbents have the potential to remove heavy metals, dyes, phenol, and phenolic derivatives from effluents due to the presence of functional groups that can bind pollutants (Kumar *et al.* 2018a, b; Kadhom *et al.* 2020; El-Bery *et al.* 2022; Haque *et al.* 2022; Jabeen *et al.* 2022; Hambisa *et al.* 2023; Sen 2023). Among the various types of agro-waste biomass that are locally and abundantly available, date palm is one of the best candidates for this study purpose.

Date palm is a highly significant fruit crop in Saudi Arabia, producing almost 1.58 million tons of dates annually, which accounts for nearly 20% of the global date production. Date fruit is made up of fruit pulp (85 to 90% w/w) and a seed or pit (10 to 15% w/w) (Li *et al.* 2020). In 2021, Saudi Arabia ranked first in the world in date exports. Across the Middle East region, the total number of date palm trees in Saudi Arabia is almost 36 million, which includes 27 million fruitful trees as of 2020. The Riyadh Region has the highest number of date palm trees in Saudi Arabia, with a total of 9 million. The region produces more than 400,000 tons of dates, which represents 24% of the Kingdom's total production (Santos Rocha *et al.* 2018; Nourani and Pegna 2022). The date pit material is not only cheap and renewable but is also considered an environmental problem in many regions, especially in Saudi Arabia and Mediterranean countries. Many studies carried out in the past few years have utilized date palm stone waste biomass (Ahmed 2016) due to its high carbon content, effectiveness, widespread availability, and low cost for removing heavy metals (Al-Ghouti *et al.* 2010; Hilal *et al.* 2012; Shafiq *et al.* 2018), dyes (El Messaoudi *et al.* 2016; Pathania *et al.* 2016), and phenolic derivative compounds (Al-Mutairi 2010; Okasha and Ibrahim 2010; Ahmed and Theydan 2012). Therefore, the usage of date palm stone agro-waste biomass as an adsorbent can be an effective and eco-friendly solution for the remediation of 2,4,6-TCP from wastewater.

This study investigated the effectiveness of date palm powder in its raw form and after chemical modification as an adsorbent for the remediation of chlorophenol compound (2,4,6-TCP). The study also examined how various operating conditions (such as initial pH, contact time, sorbent dosage, and adsorbate concentration) affect the performance of the adsorbent. Batch equilibrium studies were conducted at each stage of the study, and the samples were thoroughly characterized using a particle-size analyzer, elemental analyzer (CHN), BET surface area, SEM-EDX, FTIR, and TGA analysis, to better understand the relationship between the properties of the adsorbent and its ability to remove contaminants.

## EXPERIMENTAL

### Chemicals

The 2,4,6-trichlorophenol compound was obtained from Sigma-Aldrich (USA), and the stock solution was prepared by dissolving 1.68 g in 1000 mL of double-deionized water. For the batch experiments, diluted solutions of low concentrations ranging from 50 to 200 mg/L were prepared from the stock solution. The pH of the solution was adjusted using 0.1 M HCl and 0.1 M NaOH solutions.

### Collection and Preparation of Date-Palm Stone Biomass

Agro-waste raw date palm stones were gathered from the date palm orchards surrounding Riyadh City, Kingdom of Saudi Arabia. To remove impurities, the date palm stone (DPS) was initially washed with water and then dried for 30 h at 100 °C. The DPS was then ground using a DLC multifunctional grinder, and the resulting powder was sieved. The collected sieved powder was then subjected to ball-milling using Fritsch Pulverisette 7 Premium line, Germany, with zirconia ceramic and steel balls at 400 rpm for 24 h. Additionally, POWTEQ Laboratory's Micro Ball mill (GT300, Beijing, China) was utilized for 30 min at 1500 rpm. The raw micro ball-milled date palm stone sample was designated as RDSB.

### Chemical Modification of Raw Date-Palm Stone Biomass

The raw date palm stone biomass (RDSB) was chemically modified using a method similar to the one previously described by Xu *et al.* Yin Kuo *et al.* and Wang *et al.* with minor adjustments in reaction temperature and time (Kuo *et al.* 2015; Wang *et al.* 2016; Xu *et al.* 2016). To prepare CA-MDSB, 10 grams of RDSB were added to 300 mL of 0.7 mol/L citric acid (CA) solution and stirred at 400 rpm for 2 h at 30 °C. The date palm impregnated with CA was dehydrated at 70 °C for 24 h, then heated to 110 °C and kept for 120 min before cooling down to room temperature. The obtained chemical-modified RDSB by CA was washed with double distilled water several times to neutralize pH, remove excess CA, and finally dried at 80 °C for 24 h.

### Batch Studies

To investigate the adsorption equilibrium, batch experiments were conducted. An amber glass reagent bottle with a capacity of 125 mL was used. Inside the bottle, 0.1 g of RDSB and CA-MDSB were added into a 100 mL solution containing 2,4,6-TCP at a concentration of 50-200 mg/L. The samples were stirred using a shaking water bath at 175 rpm and kept the temperature constant at 30 ± 1 °C until the samples reached a steady state. The pH of the solution was varied from 2 to 10. To measure the concentration of 2,4,6-TCP, a UV-Vis spectrophotometer (Model: Shimadzu UV-1900, Tokyo, Japan) was used, and it was operated at a wavelength of 296 nm. To determine the sorption capacity ($q_e$, mg/g) and the removal efficiency, following equations were employed (Kumar *et al.* 2021),

$$q_e = \frac{(C_0 - C_e)V}{M} \quad (1)$$

$$Removal\ (\%) = \frac{(C_0 - C_e) \times 100}{C_0} \quad (2)$$

where $C_0$ is the 2,4,6-TCP concentration (mg/L) at time = 0, $q_e$ is the equilibrium adsorption

capacity, $C_e$ is the 2,4,6-TCP concentration (mg/L) at equilibrium, $M$ is the RDSB and CA-MDSB biomass (g), and $V$ is the volume (L) of the solution.

During batch kinetics studies, the 2,4,6-TCP sorption, $q_t$ (mg/g), at time $t$ was calculated as follows,

$$q_t = \frac{V(C_0 - C_t)}{M} \quad (3)$$

where $C_t$ is the concentration of solute (mg/L) at time, $t$ (min).

### Validation of Kinetic and Equilibrium Models

The normalized standard deviation of $\Delta q(\%)$ and the Chi-square ($\chi^2$) (Kumar *et al.* 2018a, 2019) obtained from Eqs. 4 and 5 were utilized to determine the most suitable fit of kinetics and equilibrium isotherm models. The mathematical expression for this is in the supplementary material.

### Characterization of RDSB and CA-MDSB Materials

Various techniques were employed to study the RDSB and CA-MDSB material. These techniques included particle size, elemental analysis (C, H, N), and BET analysis to determine specific surface area, pore volume, and average pore size. In addition, the FTIR method was used to identify the adsorbent's surface functional groups. SEM-EDX was utilized to analyze the biomass morphology. Thermogravimetric analysis (TGA) measures weight changes of a sample with respect to temperature and time. A detailed explanation of these techniques is in the Supplementary Material section 2.6 in the Appendix.

## RESULTS AND DISCUSSION

### Particle Size Data Analysis

The crushed samples of date palm stones (RDSB) were sieved using standard sieves to obtain uniform samples. These samples were then subjected to ball-milling to decrease their size and improve their specific surface area. Two different ball-milling strategies were used. The first strategy involved conventional ball-milling for a long duration of 24 h to achieve maximum size reduction.

The second strategy used micro ball-milling for 30 min. The particle size distribution of both strategies was analyzed and shown in Fig. 1(a-b). A significant difference in size reduction was found between the two strategies. The average particle size of the RDSB, which was initially over 180 µm, was reduced to 7.08 µm with the 24-h ball-milling strategy. However, the same sample undergoing 30-min micro ball-milling was reduced to 1.12 µm, which is 84% greater than the reduction achieved with conventional ball-milling.

These findings conclusively demonstrate that micro ball-milling is an effective technique for producing small-sized adsorbent samples that cannot be achieved through conventional ball-milling.

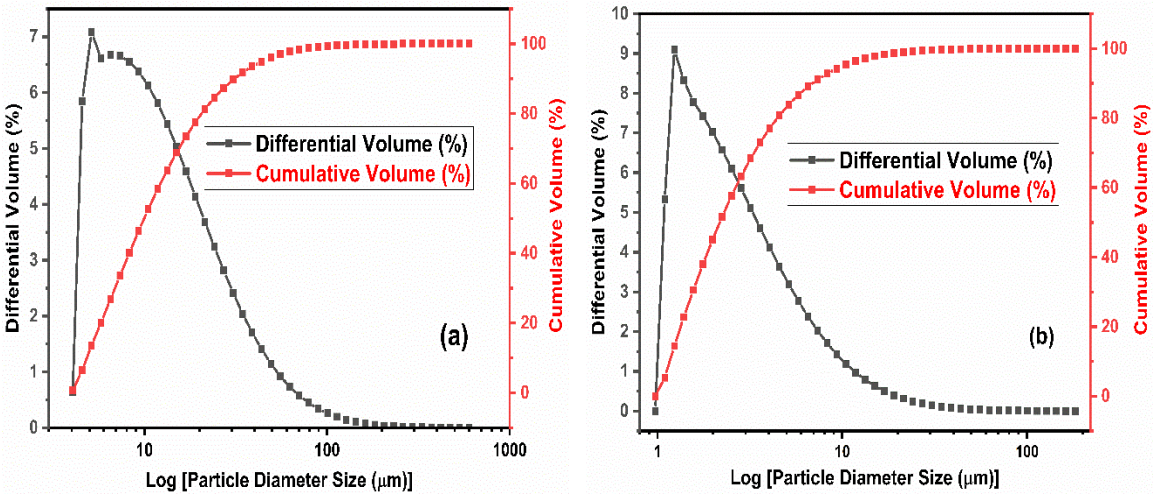


**Fig. 1(a-b).** Particle size distribution curve of (a) 24 hrs ball-milled (b) 30 min micro ball-milled date palm stone biomass (RDSB)

## Elemental (C, H, N) Analysis

The elemental composition of RDSB and CA-MDSB biomass samples, in terms of carbon, hydrogen, and nitrogen (C, H, N), is presented in Table 1. The analysis reveals that the C, H, and N content of the RDSB and CA-MDSB was similar to that of the local Sukkary date palm stones, which have 47.1% carbon, 6.63% hydrogen, and 0.9% nitrogen (Nasser *et al.* 2016). Another study that used Tunisian date-stone also reported similar values, with 46.8% C, 6.66% H, and 0.74% N (Rezma *et al.* 2019). The results indicate that the ball milling process caused less than 3% loss in the carbon content of the micro ball-milled RDSB sample, with a corresponding increase in oxygen content. This is because the fraction of other elements, *i.e.* hydrogen and nitrogen, remained unaffected during the milling process (Daffalla *et al.* 2020). After the chemical activation of the micro ball-milled biomass (RDSB) sample using citric acid, a slight decrease in the carbon, hydrogen, and nitrogen contents was observed.

**Table. 1.** Elemental Data (C, H, N) Analysis on RDSB and CA-MDSB Adsorbent

| S. No | Sample name | Carbon (%) | Hydrogen (%) | Nitrogen (%) |
|---|---|---|---|---|
| 1 | RDSB | 43.99 | 6.69 | 1.07 |
| 2 | CA-MDSB | 42.32 | 6.14 | 0.54 |

## FTIR Analysis

The FTIR spectra of RDSB, CA-MDSB, and their compositions after 2,4,6-TCP adsorption were analyzed. The bands in the range of 4000 to 400 $cm^{-1}$ were examined and shown in Fig. 2(a-d). The highest broadband peak at around 3425 $cm^{-1}$ in Fig. 2a mainly reflects the stretching vibration of hydroxyl groups (–OH) (Li *et al.* 2018). The peak at 2929 $cm^{-1}$ is assigned to the C–H stretching vibration of methyl groups. In addition, the remaining peaks are C=O (carbonyls), C=C (alkene), $CH_2$ cellulose, lignin, C-H cellulose, hemicellulose stretching vibrations at 1736, 1628, 1442, 1365, and C-O stretching 1069 $cm^{-1}$, respectively (Xu *et al.* 2016). In Fig. 2(c), spectra of the after chemical modification of CA-MDSB biomass peaks confirmed the presence of O-H, C-H stretching band vibrations at 3410 $cm^{-1}$ and 2922 $cm^{-1}$. Other peaks were due to C=O, C=C, and C-O-C, stretching vibration frequencies at 1748, 1644, and 1069 $cm^{-1}$, respectively (Yang *et al.*

2010), indicating the presence of carbonyl group, alkene functional groups. Some bands in the range 600 to 800 $cm^{-1}$ were due to the vibrations of O–H groups. After modification, the hydroxyl group peak intensity was decreased. The peak intensity of the carboxyl group significantly increased, which was evidently due to the introduction of citric acid (Gong *et al.* 2008; Wang *et al.* 2016). After adsorption, there was little and negligible change in the intensity of the spectrum peaks, as seen in Fig. 2(b and d). These changes could be attributed to specific interactions between hydroxyl and carboxyl groups with 2,4,6-TCP molecules.

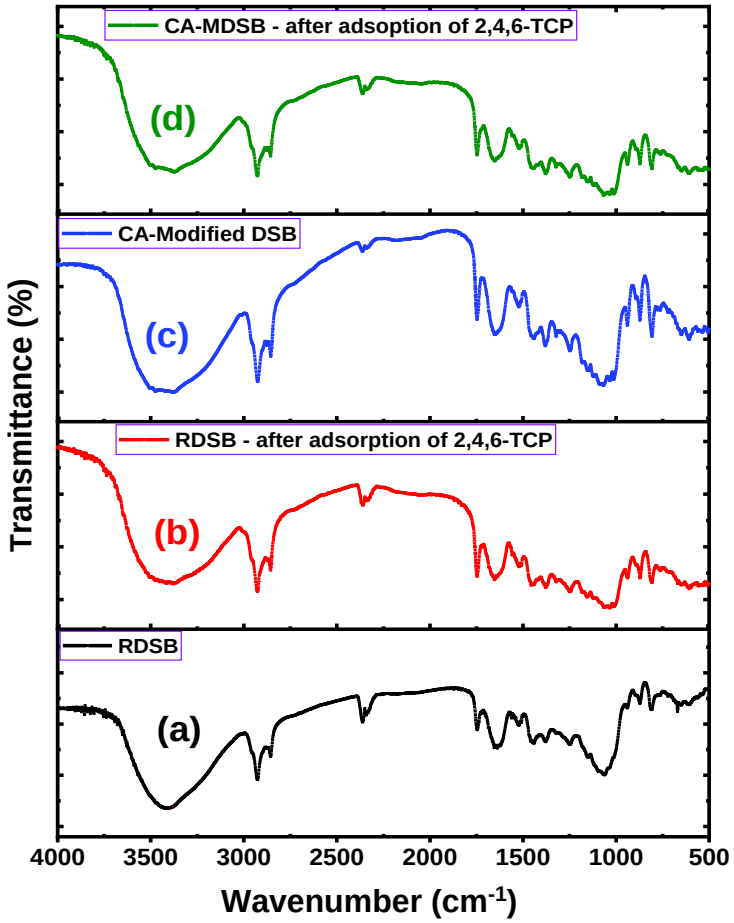


**Fig. 2.** FTIR analysis of date palm stone biomass (a) RDSB (b) RDSB–after adsorption of 2,4,6-TCP (c) CA–MDSB (d) CA–MDSB after adsorption of 2,4,6-TCP

## BET Analysis

The supplementary figures (S1 through S4) show the BET characterization of raw date-palm, 24-h ball-milled, micro ball-milled, and chemically treated with citric acid biomass samples in terms of $N_2$ adsorption/desorption isotherm curves and cumulative pore size and pore volume (Inset). The BET surface area, pore volume, and pore size for all samples are presented in Table 2. The ground DPS had the lowest surface area, pore volume, and pore size. When the raw biomass sample was subjected to 24-h ball-milling, there was a significant enhancement of the surface area in most cases, with a rather insignificant increase in the pore volume and a substantial decrease in the pore size. Using micro ball-milling further improved the specific surface area for DPS. In fact, there was almost a hundred-fold increase in the surface area for DPS after micro ball-milling, mainly

due to the reduction of the sample size. However, the pore volume showed a decrease. After micro ball-milling, the samples were subjected to chemical modification using citric acid (CA). In this case, there was a substantial reduction in the surface area since the micro ball-milled sample had 0.4574 $m^2/g$ before modification. The reduction in the surface area was accompanied by a simultaneous reduction in the pore volume, indicating the pore blockage due to the chemical modification of the micro ball-milled DPS sample (RDSB). Similar results were reported for the lowering of BET surface area in surfactant-modified montmorillonite and surface-modified lignocellulosic material (Krishna *et al.* 2000; Thamilarasi *et al.* 2018).

**Table 2.** BET data of a Grinding Sample of Date Palm, 24 h Ball-milling, and 30 min Micro Ball-milling Biomass Material

| S. No | Adsorbent | BET Surface Area ($m^2/g$) | Pore Volume ($cm^3/g$) | Pore Size (Å) |
|---|---|---|---|---|
| 1 | Ground biomass | 0.0059 | 0.0004 | 1176.8 |
| 2 | 24 hrs ball-milling | 0.1325 | 0.0005 | 332.2 |
| 3 | Micro ball-milling | 0.4574 | 0.0014 | 481.4 |
| 4 | CA–MDSB | 0.0403 | 0.00008 | 1849.58 |

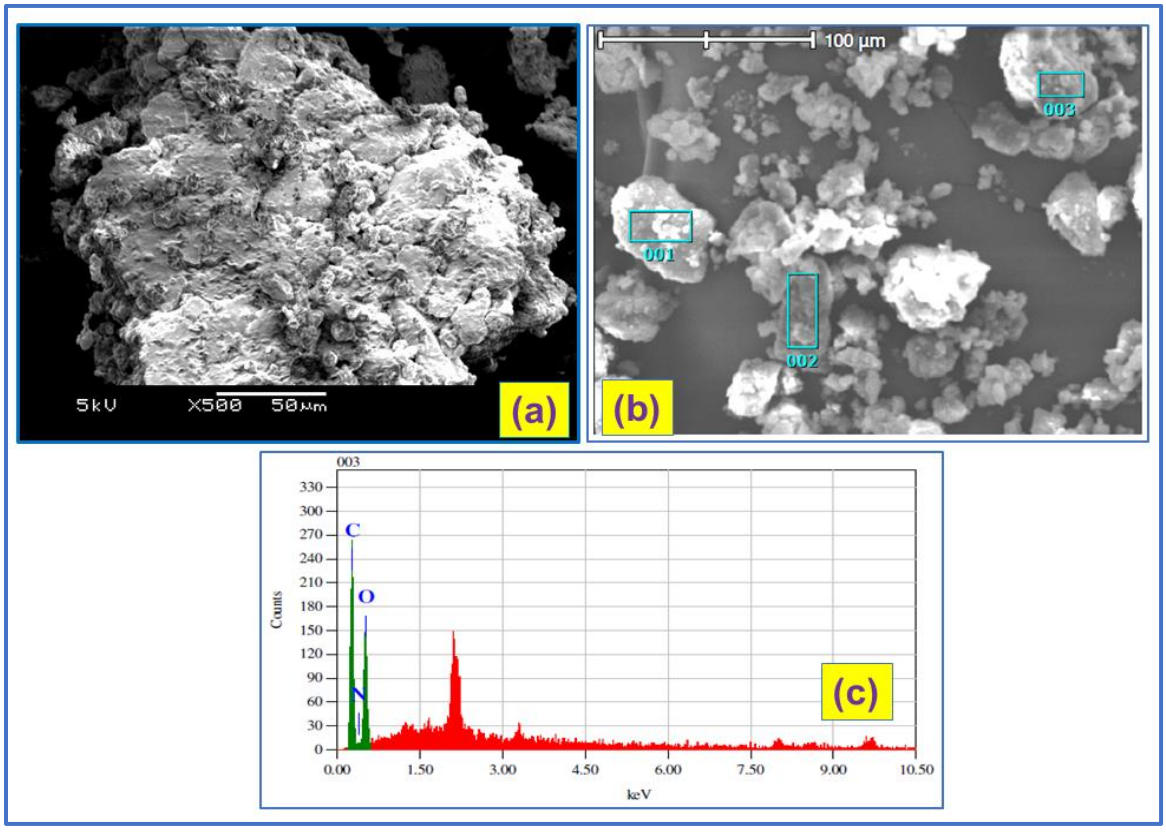


**Fig. 3.** SEM-EDX images of raw date palm stone (RDSB) biomass

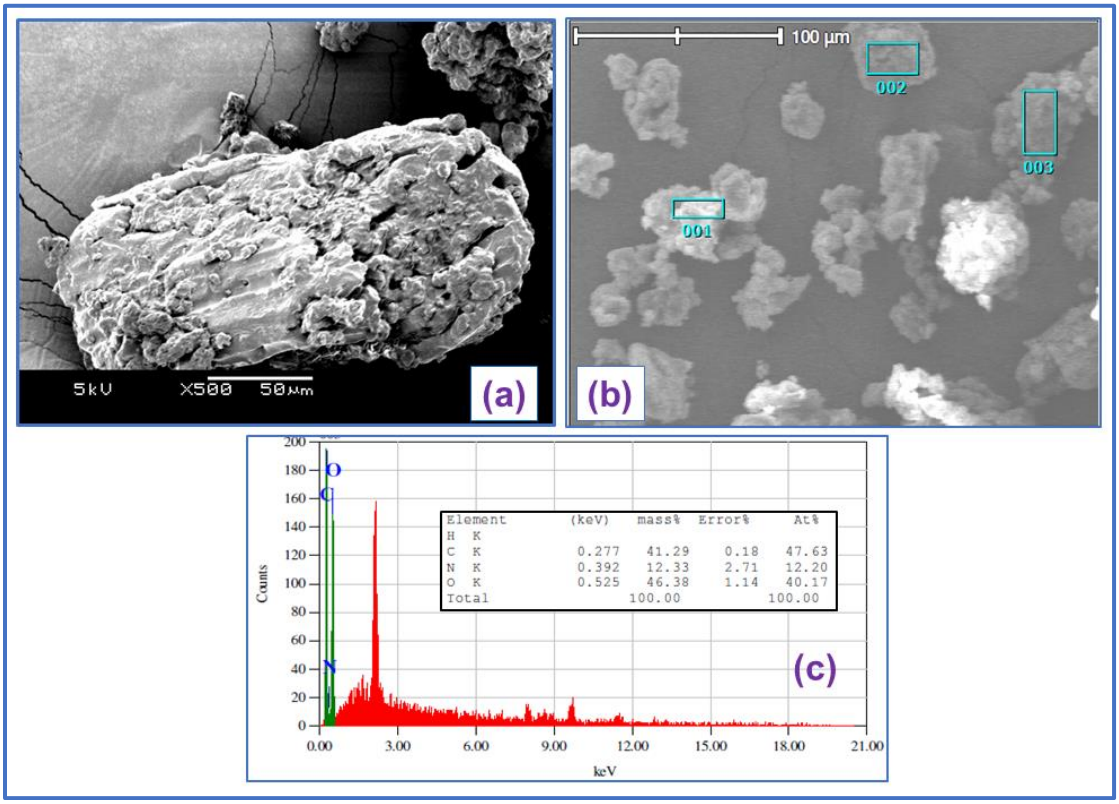


**Fig. 4.** SEM-EDX images of CA-chemical modified date palm stone (CA–MDSB) biomass

## SEM Analysis

Scanning electron microscopy shows the surface morphology of RDSB and CA-MDSB biomass. The images in Figs. 3(a) and 4(a) show particles with an irregular shape and a porous surface. Figure 3(a) shows that the morphology of the particle was bulky and irregular, with a slightly agglomerated, smooth surface. Complete separation had yet to occur, and the particles were held together by weak physical force. Figure 4(a) shows that the surface structure of the chemically modified biomass was porous, with rough surface, fracture, and contours like pores. The EDX elemental composition analysis confirmed the ultimate composition (C, H, N) of RDSB and CA-MDSB, as shown in Figs. 3, 4 (b-c). The results of the semi-quantitative analysis agreed with the elemental analysis of C, H, and N.

## Thermogravimetric Analysis (TGA)

The thermal analysis of the raw and modified date palm stone (RDSB and CA-MDSB) biomass is depicted in Fig. 5. The thermal behavior of biomass materials depends on their chemical composition, structure, and crystallinity degree. In general, decomposition of lignocellulose biomass can occur in four distinct phases, *i.e.*, i) moisture evaporation, ii) hemicellulose degradation, iii) cellulose degradation, and iv) lignin degradation (Shaikh *et al.* 2021). The temperature at the onset of decomposition can be used to evaluate stability. The first small decomposition curve at around 100 °C represented the elimination of adsorbed water or moisture content, which was nearly 3.31% and 6.07% for RDSB and CA-MDSB, respectively. Then, samples displayed thermal stability with negligible mass loss depending on the nature of the samples. The RDSB showed the temperature at the onset of decomposition at about 221 °C, while CA-MDSB samples showed it was at 240 °C. This difference could be attributed to the chemical modification of biomass. The CA-MDSB sample showed a relatively high onset degradation

temperature. The mass loss beyond 420 °C was due to the decomposition of lignin and char components, which took place over a wide temperature range, up to 600 °C. Similar results were observed in earlier reported studies (El may *et al.* 2012; Parthasarathy *et al.* 2022).

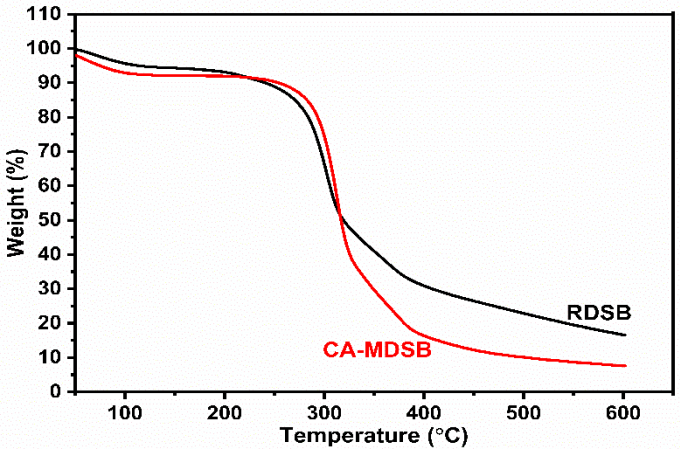


**Fig. 5.** TGA analysis of RDSB and CA–MDSB biomass

## Effect of Solution pH

The effect of pH value on the removal capacity of 2,4,6-TCP was investigated by varying the pH of the solution from 2 to 10. Figure 6 shows the pH effect on the adsorption efficiencies for RDSB and CA-MDSB. There was a strong correlation between the solution pH and the uptake capacity of 2,4,6-TCP. As illustrated in Fig. 6, the sorption capacity of both adsorbents for 2,4,6-TCP increased as the pH of the solution increased from 2 to 7. However, when the pH was increased beyond 7, the sorption capacity decreased. This is because 2,4,6-TCP is a weak acid with a dissociation constant of 6.23, so an acidic pH below this value helps it remain un-dissociated, and dispersion interactions become more effective (Kumar *et al.* 2019). The maximum adsorption of 2,4,6-TCP on RDSB and CA-MDSB was observed at pH values of 6.0 and 7.0, respectively. Recent studies have shown that similar behavior occurs during the adsorption of 2,4,6-TCP on agro waste adsorbents (Kuśmierek *et al.* 2017; Kumar *et al.* 2018b; Ahmad *et al.* 2023). Thus, experiments for 2,4,6-TCP were conducted at pH 6.0 and 7.0 on RDSB and CA-MDSB, respectively.

## Effect of RDSB and CA-MDSB Dosage

The amount of sorbent used in the adsorption process is an essential factor in determining its effectiveness. To examine the impact of sorbent dosage, experiments were conducted by varying the dosage of sorbent from 0.1 to 1.0 g in 100 mL of a test solution containing 100 mg/L of 2,4,6-TCP at an optimum pH of 6.0 and 7.0 for 4 h at a temperature of 30 ± 1 °C. Results shown in Fig. 7(a-b) indicated that the removal percentage of 2,4,6-TCP increased from 80.9% to 87.5% and 83.8% to 94.0% with an increasing amount of RDSB and CA-MDSB dosage, respectively. This is due to the presence of more active sites on the surface of the adsorbent, which makes it easier for 2,4,6-TCP molecules to penetrate into these sites. However, the sorption capacity of RDSB and CA-MDSB for 2,4,6-TCP molecules decreased significantly. This may be due to the agglomeration of the adsorbent or interactions between sorbent atoms, which reduces the availability of active sorption sites (Kumar *et al.* 2021; Siva Kumar *et al.* 2023). Additionally, there was hardly any improvement in the removal efficiency of 2,4,6-TCP beyond 0.6 and 0.5 g/L of RDSB and CA-MDSB, respectively.

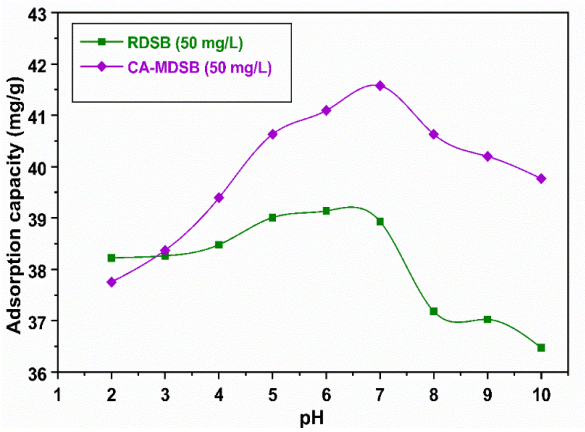


**Fig. 6.** Effect of pH on 2,4,6-TCP adsorption onto (a) RDSB and (b) CA–MDSB at 30±1ºC ($C_0$ = 50 mg/L, Contact time = 4h, adsorbent dosage = 0.1 g, Agitation speed = 175 rpm)

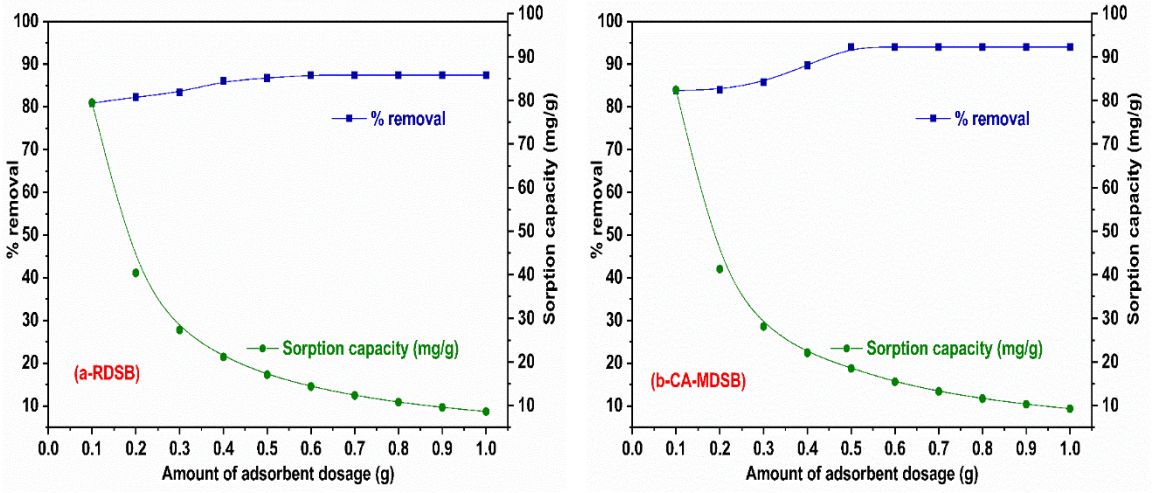


**Fig. 7 (a-b).** 2,4,6-TCP adsorption onto (a) RDSB at pH = 6.0 (b) CA–MDSB at pH = 7.0 of adsorbent dosage level at 30±1ºC [$C_0$ = 100 mg/L, Sorbent dosage = 0.1 – 1.0 g, Agitation speed = 175 rpm, Contact time = 4h]

## Effect of Contact Time and Initial Concentration

The time for agitation plays a critical role in determining the amount of pollutant taken up by the adsorbent. At a temperature of 30 °C, the impact of contact duration and initial 2,4,6-TCP concentration (ranging from 50 to 200 mg/L) was measured on 2,4,6-TCP uptake. As shown in Fig. 8(a-b), the absorption capacity increased with time and initial concentration. The sorption rate was initially fast until an equilibrium constant was reached. For RDSB and CA-MDSB, this occurred after 150 and 120 min of contact, respectively. The fast absorption rate at the beginning of sorption was attributed to the greater affinity of the interacting groups and the availability of the adsorbent's external surface. As shown in Fig. 8(a-b), the equilibrium sorption capacity ($q_e$) increased from 28.58 to 140.47 and 30.36 to 157.06 mg/g as the initial concentrations of 2,4,6-TCP increased from 50 to 200 mg/L. The higher initial concentrations resulted in increased mass transfer driving force, leading to greater 2,4,6-TCP adsorption. As a result, the RDSB and CA-MDSB contact time for the batch experimental studies was set at 150 and 120 min, respectively.

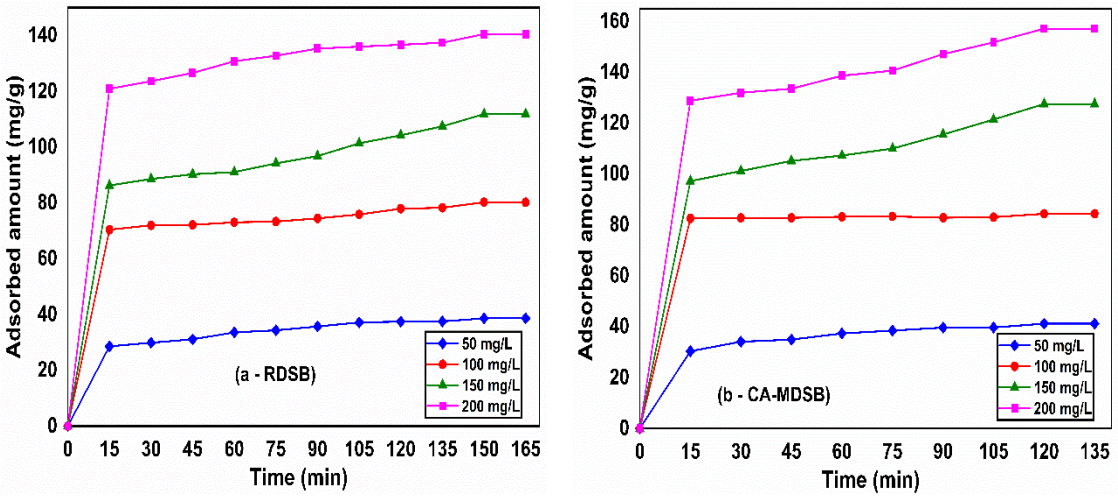


**Fig. 8 (a-b).** Effect of 2,4,6-TCP adsorption onto (a) RDSB at pH = 6.0 and (b) CA–MDSB at pH = 7.0, contact time at 30±1ºC [(◆) $C_0$= 50 mg/L, (●) $C_0$= 100 mg/L, (▲) $C_0$= 150 mg/L, (■) $C_0$= 200 mg/L; adsorbent dosage = 0.1g; Contact time = 165 & 135 min, Agitation speed = 175 rpm]

## Adsorption Kinetics

The pseudo-first-order (PFO) and pseudo-second-order (PSO) kinetic models can predict the rate of contaminants adsorption onto RDSB and CA-MDSB. To understand the adsorption mechanism, the data was fitted using PFO and PSO models (Dada *et al.* 2021). Equations 6 and 7 in the supplementary section text 3.9 represent the models. Table 3 shows the kinetic results for the adsorption of 2,4,6-TCP by RDSB and CA-MDSB adsorbents. Additionally, $q_{e\ (exp)}$ is displayed to compare with the corresponding predicted values. The PSO model was found to provide better agreement in RDSB and CA-MDSB between experimental values and model predictions of $q_e$, in the range of initial 2,4,6-TCP concentration ($C_0$ = 50 to 200 mg/L) considered in the study. The results confirmed that the CA-MDSB was more effective in adsorbing 2,4,6-TCP than the RDSB adsorbent.

The Elovich and IPD (Intraparticle diffusion) models (Kumar *et al.* 2009; Siva Kumar *et al.* 2012a) have been utilized to explain the adsorption kinetics. The Elovich equation is used to calculate the contaminant uptake rate. However, the model does not suggest any clear mechanism governing the interaction between adsorbent and adsorbate; instead, it assumes that the adsorbent surfaces are energetically heterogeneous. However, from Table 3, the calculated $q_e$ values of the Elovich model do not show good agreement with experimental equilibrium values. On the other hand, the IPD model evaluates the relative significance of the intra-particle diffusion in the mass transport of the solute and calculates the $k_{id}$ values. As seen in Table 3, the RDSB and CA-MDSB intercept ranged from 23.20 to 111.87 and 25.26 to 112.61, respectively. Therefore, the intra-particle diffusion model was not valid in this case since a large intercept indicates that adsorption primarily occurs on the adsorbent surface, and the mass transport is controlled by external mass transport resistance throughout the movement of the solute from the liquid phase to the external surface of the adsorbent.

The study compared the predictions of experimental and calculated data models for 2,4,6-TCP concentrations ranging from 50 to 200 mg/L using PFO, PSO, Elovich Kinetic, and Intraparticle diffusion equations. Supplementary Figures S5(a–d) and S6(e–h) depict the comparison results. Based on the data presented in Figs. S5 and S6, it can be concluded that the PSO kinetic model accurately predicted the adsorption of 2,4,6-TCP onto RDSB and CA-MDSB. However, the PFO kinetics did not provide a satisfactory description of

the same process. The results fitted with PFO, PSO, Elovich, and IPD kinetic models of 2,4,6-TCP adsorption onto RDSB and CA-MDSB, their corresponding regression ($R^2$), Chi-square ($\chi^2$) and $\Delta q_t$ (%) values are listed in Table 3 and 4. The $R^2$ value for the PSO model was found to be greater than 0.993 to 0.999 and 0.993 to 1 for RDSB and CA-MDSB, respectively, which was much closer to unity than those of the PFO, Elovich, and IPD models. The calculated ($q_e$, cal) values for RDSB and CA-MDSB showed an excellent fit with the experimental values ($q_t$, exp) for the PSO kinetic model. The Chi-square ($\chi^2$) values ranged from 0.98 to 5.58 and from 0 to 2.64% for RDSB and CA-MDSB, respectively, indicating that the PSO model provided the best fit. Based on the investigative results, it appears that the PSO is more suitable option for adsorbing 2,4,6-TCP on RDSB and CA-MDSB. This result is consistent with recent studies that have reported similar kinetics of 2,4,6-TCP adsorption on other adsorbents, following the PSO kinetic model (Ahmad *et al.* 2023; Hyder *et al.* 2023; Nazal *et al.* 2021; Soltani Goharrizi *et al.* 2019).

## Adsorption Isotherm Models

This study focused on three different empirical models: the Langmuir (Eq.10), Freundlich (Eq. 11), and Dubinin–Radushkevich (Eq. 13) models (Dubinin, M. M. and Radushkevich 1947; Freundlich 1906; Langmuir 1917). The equilibrium adsorption isotherm was analyzed using these models and detailed information is provided in the supplementary section. The Langmuir isotherm provides information on the maximum amount of solute that can be adsorbed per unit mass of the sorbent, and is concerned with adsorption energy. The Freundlich isotherm model can be used to correlate heterogeneous surfaces containing binding sites to their different energies. The Dubinin–Radushkevich isotherm has also been utilized to model the present equilibrium data. For adsorption by ion exchange, the value of $E$ usually lies between 8 and 16 kJ/mol, while it is less than 8 kJ/mol for the case of physical adsorption. Correlation coefficients, parameter values, normalized standard deviation ($\Delta q_t$ (%)) and Chi-square ($\chi^2$) for all three isotherms, *i.e.*, Langmuir, Freundlich, and D-R, are presented in Table 5 for comparison. In this study, the experimental data and predictions from three isotherm models (Langmuir, Freundlich, and D-R) were compared in supplementary Fig. S7(a-b). The Langmuir isotherm resulted in higher $R^2$ values (0.9996 and 0.9992) for RDSB and CA-MDSB, lower $\Delta q_t$ (3.88 and 6.09%), and lower Chi-square ($\chi^2$) values (0.86 and 2.19). The Langmuir model provided a better fit for the experimental sorption data for RDSB and CA-MDSB than the Freundlich and D-R models. To compare this study with other studies, Table 6 summarizes the data of 2,4,6-TCP adsorption systems with different types of adsorbents.

## Adsorption Mechanism

The adsorption process of 2,4,6-TCP onto raw (RDSB) and modified date palm stone biomass (CA-MDSB) may involve various mechanisms, such as ion exchange, surface complexation, and electrostatic interactions. In addition, the excellent fits of the kinetic data to the PSO equation, as shown earlier, implies that the rates of adsorption were controlled by a process of adsorption into a network of small pores (Hubbe *et al.* 2019). The FTIR data analysis (Fig. 2) indicates that the biomass surface contains different functional groups, such as hydroxyl, carbonyl, alkene, cellulose, lignin, hemicellulose carboxyl, and amine groups, which play an essential role in the sorption process.

**Table 3.** PFO and PSO Kinetic Parameters of 2,4,6-TCP on RDSB and CA-MDSB

| 2,4,6-TCP–Raw Date Palm Stone Biomass (RDSB) | | | | | | | | | | | |
|---|---|---|---|---|---|---|---|---|---|---|---|
| PFO Kinetic Model | | | | | | | PSO Kinetic Model | | | | |
| Conc (mg/L) | $q_{e,\ exp}$ (mg/g) | $q_{e,\ cal}$ (mg/g) | $k_1$ ($min^{-1}$) | $R^2$ | $\Delta q_t$ (%) | $\chi^2$ | $q_{e,\ cal}$ (mg/g) | $k_2$ (g/mg/min) | $R^2$ | $\Delta q_t$ (%) | $\chi^2$ |
| 50 | 38.60 | 16.59 | 0.020 | 0.964 | 63.76 | 443.15 | 40.19 | 0.002 | 0.997 | 6.28 | 1.07 |
| 100 | 80.23 | 14.27 | 0.013 | 0.866 | 84.41 | 6097.51 | 79.47 | 0.003 | 0.998 | 4.36 | 1.22 |
| 150 | 111.79 | 39.39 | 0.013 | 0.875 | 73.51 | 2665.38 | 110.91 | 0.001 | 0.993 | 8.02 | 5.58 |
| 200 | 140.47 | 26.32 | 0.016 | 0.987 | 82.72 | 8362.60 | 141.08 | 0.001 | 0.999 | 3.04 | 0.98 |
| 2,4,6-TCP–CA-Modified Date Palm Stone Biomass (CA-MDSB) | | | | | | | | | | | |
| 50 | 41.17 | 15.45 | 0.023 | 0.978 | 77.36 | 500.78 | 42.41 | 0.003 | 0.998 | 3.33 | 0.22 |
| 100 | 84.36 | 1.97 | 0.005 | 0.983 | 107.29 | 116142 | 83.40 | 0.047 | 1 | 0.26 | 0.00 |
| 150 | 127.50 | 44.61 | 0.015 | 0.869 | 83.57 | 2374.63 | 125.35 | 0.001 | 0.993 | 6.27 | 2.64 |
| 200 | 157.06 | 44.86 | 0.017 | 0.871 | 87.81 | 4073.95 | 156.01 | 0.001 | 0.995 | 5.67 | 2.81 |

**Table 4.** IDM and EKM Kinetic Parameters of 2,4,6-TCP on RDSB and CA-MDSB

| Intraparticle Diffusion Model (IDM) | | | | | | | Elovich Kinetic Model (EKM) | | | | | | |
|---|---|---|---|---|---|---|---|---|---|---|---|---|---|
| 2,4,6-TCP–Raw Date Palm Stone Biomass (RDSB) | | | | | | | | | | | | | |
| Conc (mg/L) | $q_{e,\ exp}$ (mg/g) | $q_{e,\ cal}$ (mg/g) | $k_{id}$ | $C$ | $R^2$ | $\Delta q_t$ (%) | $\chi^2$ | $q_{(e,\ cal)}$ (mg/g) | $(1/b)\ln(ab)$ (mg/g) | $1/b$ (mg/g) | $R^2$ | $\Delta q_t$ (%) | $\chi^2$ |
| 50 | 38.60 | 38.21 | 1.29 | 23.20 | 0.977 | 1.35 | 0.06 | 37.49 | 14.98 | 4.58 | 0.947 | 2.43 | 0.15 |
| 100 | 80.23 | 77.45 | 0.99 | 65.87 | 0.906 | 0.91 | 0.07 | 76.80 | 60.04 | 3.41 | 0.818 | 1.21 | 0.14 |
| 150 | 111.79 | 104.58 | 2.72 | 72.93 | 0.913 | 2.04 | 0.40 | 102.75 | 57.29 | 9.26 | 0.812 | 2.84 | 0.86 |
| 200 | 140.47 | 138.76 | 2.31 | 111.87 | 0.974 | 0.62 | 0.06 | 137.55 | 96.75 | 8.31 | 0.967 | 0.87 | 0.08 |
| 2,4,6-TCP – CA-Modified Date Palm Stone Biomass (CA-MDSB) | | | | | | | | | | | | | |
| 50 | 41.17 | 40.49 | 1.48 | 25.26 | 0.969 | 1.69 | 0.06 | 39.96 | 16.91 | 4.95 | 0.983 | 1.22 | 0.03 |
| 100 | 84.36 | 83.27 | 0.11 | 82.06 | 0.981 | 0.04 | 0.00 | 83.22 | 81.44 | 0.38 | 0.949 | 0.07 | 0.00 |
| 150 | 127.50 | 118.14 | 3.55 | 81.74 | 0.941 | 1.79 | 0.22 | 116.47 | 63.83 | 11.30 | 0.872 | 2.65 | 0.48 |
| 200 | 157.06 | 148.73 | 3.52 | 112.61 | 0.922 | 1.66 | 0.23 | 146.98 | 95.27 | 11.11 | 0.838 | 2.39 | 0.48 |

**Table 5.** Isotherm Parameters of 2,4,6-TCP on RDSB and CA-MDSB

| Adsorbate | Langmuir | | | | | Freundlich | | | | | Dubinin- Radushkevich | | | | |
|---|---|---|---|---|---|---|---|---|---|---|---|---|---|---|---|
| | $q_m$ (mg/g) | $b$ (L/mg) | $R^2$ | $\Delta q_e$ (%) | $X^2$ | $K_F$ ((mg/g)(L/mg)$^{1/n}$) | $n$ | $R^2$ | $\Delta q_e$ (%) | $X^2$ | $q_s$ (mmol/g) | $E$ (kJ/mol) | $R^2$ | $\Delta q_e$ (%) | $X^2$ |
| RDSB | | | | | | | | | | | | | | | |
| 2,4,6-TCP | 53.7 | 0.033 | 0.9996 | 3.88 | 0.86 | 0.975 | 0.675 | 0.9852 | 9.78 | 2.88 | 1.63 | 6.47 | 0.9788 | 11.74 | 4.21 |
| CA-MDSB | | | | | | | | | | | | | | | |
| 2,4,6-TCP | 123.8 | 0.026 | 0.9992 | 6.09 | 2.19 | 2.781 | 0.828 | 0.9990 | 2.34 | 0.16 | 2.66 | 7.25 | 0.9970 | 4.10 | 0.45 |

**Table 6.** The Maximum Sorption Capacities $Q_0$ (mg/g) of Different Adsorbents and the Remediation Process of 2,4,6-TCP on RDSB and CA-MDSB Experimental Conditions

| Adsorbent | $Q^0$ (mg/g) | Experimental Conditions | | References |
|---|---|---|---|---|
| | | pH | Contact time | |
| *Sargassum boveanum* Macroalgae (MA)<br>Biochar derived MA (BCM) | 10.0<br>175.0 | 5 | 6 hr<br>6 hr | (Nazal *et al.* 2021) |
| Pine bark powder | 142.8 | 6 | 2 hr | (Kumar *et al.* 2018b) |
| Azollafiliculoides biomass | 6.2 | 5 | 2 hr | (Ali *et al.* 2013) |
| *Acacia leucocephala* bark | 256.4 | 5 | 3 hr | (Siva Kumar *et al.* 2012a) |
| *Canna indica* | 52.9 | 4 | 20 days | (Enyoh and Isiuku 2021) |
| Bentonite modified with benzyl dimethyl tetra decyl ammonium chloride | 35.0 | 4 | 1 | (Ghezali *et al.* 2019) |
| Chemically modified chitosan CS-SA-CD | 375.9 | 5 | 1.5 hr | (Zhou *et al.* 2014) |
| RDSB | 53.7 | 6 | 2.5 hr | This study |
| CA-MDSB | 123.8 | 7 | 2 hr | This study |

After adsorption, the frequency of functional groups at RDSB and CA-MDSB were slightly changed due to the adsorption of 2,4,6-TCP molecules, showing a chemical interaction between adsorbate and surface functional groups of the adsorbent. The kinetic and isotherm model provide different insights into the mechanism of adsorption on the adsorbent. The D-R Isotherm suggests that the mechanism for 2,4,6-TCP adsorption is physisorption (H-bonding and van der Waals dispersion forces), while the PSO kinetics data model indicates that the adsorption mechanism can also be attributed to rates of diffusion (Hubbe *et al*. 2019).

## CONCLUSIONS

1. The initial average particle size of raw date palm stone biomass (RDSB) was above 180 µm. After 24 h of ball-milling, the size was reduced to 7.08 µm. Further, the sample underwent 30-min micro ball-milling, which resulted in a reduction to 1.12 µm. This reduction was 84% greater than what was achieved with conventional ball-milling.
2. The adsorption process of 2,4,6-TCP onto RDSB and citric acid modified date palm stone biomass (CA-MDSB) showed fast remediation at the initial stage, with equilibrium achieved within 150 and 120 min of contact time, respectively. A pH of 6 and 7 was found to be the optimal pH level.
3. For 2,4,6-trichlorophenol (2,4,6-TCP), the CA-MDSB achieved a removal efficiency that was up to 94% at 0.5 g/L, whereas the RDSB attained an 87% removal efficiency at 0.6 g/L.
4. The PSO kinetic model was the most suitable for representing the sorption kinetics of RDSB and CA-MDSB biomass.
5. The Langmuir model predicted a maximum uptake sorption capacity of 53.7 and 123.8 mg/g at 30 ± 1 °C for RDSB and CA-MDSB, respectively.
6. The results of the experiment indicated that CA-MDSB had a higher capacity for adsorption and removal of 2,4,6-TCP.
7. Based on these findings, date palm stone biomass can be used as an eco-friendly and easily available for the effective remediation of 2,4,6-TCP from aqueous wastewater.

### Funding

This project was funded by the National Plan for Science, Technology, and Innovation (MAARIFAH), King Abdulaziz City for Science and Technology, Kingdom of Saudi Arabia, Award Number (2-17-01-001-0064).

## ACKNOWLEDGMENTS

This project was funded by the National Plan for Science, Technology, and Innovation (MAARIFAH), King Abdulaziz City for Science and Technology, Kingdom of Saudi Arabia, Award Number (2-17-01-001-0064).

## REFERENCES CITED

Abdulrahman, M. S., Alsarayreh, A. A., Barno, S. K. A., Abd Elkawi, M. A., and Abbas, A. S. (2023). "Activated carbon from sugarcane as an efficient adsorbent for phenol from petroleum refinery wastewater: Equilibrium, kinetic, and thermodynamic study," *Open Engineering* 13(1), article 20220442. DOI: 10.1515/eng-2022-0442

Ahmad, S., Mun, H., Zhang, M., Yang, X., Gao, F., and Tang, J. (2023). "Mechanistic details of the removal of 2,4,6-trichlorophenol from aqueous solution by iron and nitrogen co-doped biochar: Characterization, performance, and mechanism studies," *Separation and Purification Technology* 332, article 125750. DOI: 10.1016/j.seppur.2023.125750

Ahmaruzzaman, M. (2008). "Adsorption of phenolic compounds on low-cost adsorbents: A review," *Advances in Colloid and Interface Science* 143, 48-67. DOI: 10.1016/j.cis.2008.07.002

Ahmed, M. J. (2016). "Preparation of activated carbons from date (*Phoenix dactylifera* L.) palm stones and application for wastewater treatments: Review," *Process Safety and Environmental Protection* 102, 168-182. DOI: 10.1016/j.psep.2016.03.010

Ahmed, M. J., and Theydan, S. K. (2012). "Equilibrium isotherms, kinetics and thermodynamics studies of phenolic compounds adsorption on palm-tree fruit stones," *Ecotoxicology and Environmental Safety* 84, 39-45. DOI: 10.1016/j.ecoenv.2012.06.019

Al-Ghouti, M. A., Li, J., Salamh, Y., Al-Laqtah, N., Walker, G., and Ahmad, M. N. M. (2010). "Adsorption mechanisms of removing heavy metals and dyes from aqueous solution using date pits solid adsorbent," *Journal of Hazardous Materials* 176, 510-520. DOI: 10.1016/j.jhazmat.2009.11.059

Al-Mutairi, N.Z. (2010). "2,4-Dinitrophenol adsorption by date seeds: Effect of physico-chemical environment and regeneration study," *Desalination* 250, 892-901. DOI: 10.1016/j.desal.2008.10.035

Ali, M., Balarak, D., and Mahdavi, Y. (2013). "Application of azolla for 2,4,6-trichlorophenol (TCP) removal from aqueous solutions," *Archives of Hygiene Sciences* 2, 143-149.

Baker, M. D., Mayfield, C. I., and Inniss, W. E. (1980). "Degradation of chlorophenols in soil, sediment and water at low temperature," *Water Research* 14, 1765-1771. DOI: 10.1016/0043-1354(80)90112-8

Crini, G., Lichtfouse, E., Wilson, L.D., and Morin-Crini, N. (2019). "Conventional and non- conventional adsorbents for wastewater treatment," *Environmental Chemistry Letters* 17, 195-213. DOI: 10.1007/s10311-018-0786-8

Dada, A. O., Adekola, F. A., Odebunmi, E. O., Ogunlaja, A. S., and Bello, O. S. (2021). "Two-three parameters isotherm modeling, kinetics with statistical validity, desorption and thermodynamic studies of adsorption of Cu(II) ions onto zerovalent iron nanoparticles," *Scientific Reports* 11, 1-15. DOI: 10.1038/s41598-021-95090-8

Daffalla, S. B., Mukhtar, H., and Shaharun, M. S. (2020). "Preparation and characterization of rice husk adsorbents for phenol removal from aqueous systems," *PLoS ONE* 15(12), article e0243540. DOI: 10.1371/journal.pone.0243540

Dehghani, M. H., Ahmadi, S., Ghosh, S., Othmani, A., Osagie, C., Meskini, M., AlKafaas, S. S., Malloum, A., Khanday, W. A., Jacob, A. O., Gökkuş, Ö., Oroke, A., Martins Chineme, O., Karri, R. R., and Lima, E. C. (2023). "Recent advances on sustainable adsorbents for the remediation of noxious pollutants from water and

wastewater: A critical review," *Arabian Journal of Chemistry* 16(12), article 105303. DOI: 10.1016/j.arabjc.2023.105303

Dubinin, M. M., and Radushkevich, L. V. (1947). "The equation of the characteristic curve of activated charcoal," *Proc. Acad. Sci. USSR Phys. Chem. Sect.* 55(1947), 327-329 and 331.

El-Bery, H. M., Saleh, M., El-Gendy, R. A., Saleh, M. R., and Thabet, S. M. (2022). "High adsorption capacity of phenol and methylene blue using activated carbon derived from lignocellulosic agriculture wastes," *Scientific Reports* 12, 1-17. DOI: 10.1038/s41598-022-09475-4

El may, Y., Jeguirim, M., Dorge, S., Trouvé, G., and Said, R. (2012). "Study on the thermal behavior of different date palm residues: Characterization and devolatilization kinetics under inert and oxidative atmospheres," *Energy* 44(1), 702-709. DOI: 10.1016/j.energy.2012.05.022

El Messaoudi, N., El Khomri, M., Bentahar, S., Dbik, A., Lacherai, A., and Bakiz, B. (2016). "Evaluation of performance of chemically treated date stones: Application for the removal of cationic dyes from aqueous solutions," *Journal of the Taiwan Institute of Chemical Engineers* 67, 244-253. DOI: 10.1016/j.jtice.2016.07.024

Enyoh, C. E., and Isiuku, B. O. (2021). "2,4,6-Trichlorophenol (TCP) removal from aqueous solution using *Canna indica* L.: Kinetic, isotherm and thermodynamic studies," *Chemistry and Ecology* 37, 64-82. DOI: 10.1080/02757540.2020.1821673

Freundlich, H. M. F. (1906). "Over the adsorption in solution," *J. Phys. Chem*, 57(385471), 1100-1107.

Ghezali, S., Mahdad-Benzerdjeb, A., Ameri, M., and Bouyakoub, A. Z. (2019). "Adsorption of 2,4,6-trichlorophenol on bentonite modified with benzyldimethyltetradecylammonium chloride," *Chemistry Int.* 4, 24-32.

Gong, R., Zhong, K., Hu, Y., Chen, J., and Zhu, G. (2008). "Thermochemical esterifying citric acid onto lignocellulose for enhancing methylene blue sorption capacity of rice straw," *Journal of Environmental Management* 88, 875-880. DOI: 10.1016/j.jenvman.2007.04.004

Grace Pavithra, K., Sundar Rajan, P., Arun, J., Brindhadevi, K., Hoang Le, Q., and Pugazhendhi, A. (2023). "A review on recent advancements in extraction, removal and recovery of phenols from phenolic wastewater: Challenges and future outlook," *Environmental Research* 237, article 117005. DOI: 10.1016/j.envres.2023.117005

Hambisa, A. A., Regasa, M. B., Ejigu, H. G., and Senbeto, C. B. (2023). "Adsorption studies of methyl orange dye removal from aqueous solution using Anchote peel-based agricultural waste adsorbent," *Applied Water Science* 13, 1-11. DOI: 10.1007/s13201-022-01832-y

Haque, A. N. M. A., Sultana, N., Sayem, A. S. M., and Smriti, S. A. (2022). "Sustainable adsorbents from plant-derived agricultural wastes for anionic dye removal: A review," *Sustainability (Switzerland)* 14. DOI: 10.3390/su141711098

Hilal, N. M., Ahmed, I. A., and El-Sayed, R. E. (2012). "Activated and nonactivated date pits adsorbents for the removal of copper(II) and cadmium(II) from aqueous solutions," *ISRN Physical Chemistry* 2012, 1-11. DOI: 10.5402/2012/985853

Ho, S. (2022). "Low-cost adsorbents for the removal of phenol/phenolics, pesticides, and dyes from wastewater systems: A review," *Water (Switzerland)* 14. DOI: 10.3390/w14203203

Hubbe, M. A., Azizian, S., and Douven, S. (2019). "Implications of apparent pseudo-second-order adsorption kinetics onto cellulosic materials. A review," BioResources

14(3), 7582-7626. DOI: 10.15376/biores.14.3.7582-7626

Hyder, A., Thebo, M., Janwery, D., Buledi, J.A., Chandio, I., Khalid, A., Al-Anzi, B. S., Almukhlifi, H. A., Thebo, K. H., Memon, F. N., Memon, A. A., Solangi, A. R., and Memon, S. (2023). "Fabrication of para-dimethylamine calix[4]arene functionalized self-assembled graphene oxide composite material for effective removal of 2,4,6-tri-cholorphenol from aqueous environment," *Heliyon* 9, article e19622. DOI: 10.1016/j.heliyon.2023.e19622

Jabeen, A., Kamran, U., Noreen, S., Park, S. J., and Bhatti, H. N. (2022). "Mango seed-derived hybrid composites and sodium alginate beads for the efficient uptake of 2,4,6-trichlorophenol from simulated wastewater," *Catalysts* 12. DOI: 10.3390/catal12090972

Kadhom, M., Albayati, N., Alalwan, H., and Al-Furaiji, M. (2020). "Removal of dyes by agricultural waste," *Sustainable Chemistry and Pharmacy* 16, article 100259. DOI: 10.1016/j.scp.2020.100259

Krishna, B. S., Murty, D. S. R., and Jai Prakash, B. S. (2000). "Thermodynamics of chromium(VI) anionic species sorption onto surfactant-modified montmorillonite clay," *Journal of Colloid and Interface Science* 229, 230-236. DOI: 10.1006/jcis.2000.7015

Kumar, N. S., Asif, M., and Al-Hazzaa, M. I. (2018a). "Adsorptive removal of phenolic compounds from aqueous solutions using pine cone biomass: Kinetics and equilibrium studies," *Environmental Science and Pollution Research* 25, 21949-21960. DOI: 10.1007/s11356-018-2315-5

Kumar, N. S., Asif, M., Al-Hazzaa, M. I., and Ibrahim, A. A. (2018b). "Biosorption of 2,4,6-trichlorophenol from aqueous medium using agro-waste: Pine (*Pinus densiflora* Sieb) bark powder," *Acta Chimica Slovenica* 65, 221-230. DOI: 10.17344/acsi.2017.3886

Kumar, N. S., Asif, M., Poulose, A. M., Suguna, M., and Al-Hazza, M. I. (2019). "Equilibrium and kinetic studies of biosorptive removal of 2,4,6-trichlorophenol from aqueous solutions using untreated agro-waste pine cone biomass," *Processes* 7. DOI: 10.3390/pr7100757

Kumar, N.S., and Min, K. (2011). "Removal of phenolic compounds from aqueous solutions by biosorption onto *Acacia leucocephala* bark powder: Equilibrium and kinetic studies," *Journal of the Chilean Chemical Society* 56, 539-545. DOI: 10.4067/s0717-97072011000100004

Kumar, N. S., Shaikh, H. M., Asif, M., and Al-Ghurabi, E. H. (2021). "Engineered biochar from wood apple shell waste for high-efficient removal of toxic phenolic compounds in wastewater," *Scientific Reports* 11. DOI: 10.1038/s41598-021-82277-2

Kumar, N. S., Subbaiah, M. V., Reddy, A. S., and Krishnaiah, A. (2009). "Biosorption of phenolic compounds from aqueous solutions onto chitosan-abrus precatorius blended beads," *Journal of Chemical Technology and Biotechnology* 84(7), 972-981. DOI: 10.1002/jctb.2120

Kumar, N. S., Suguna, M., Subbaiah, M. V., Reddy, A. S., Kumar, N. P., and Krishnaiah, A. (2010). "Adsorption of phenolic compounds from aqueous solutions onto chitosan-coated perlite beads as biosorbent," *Industrial and Engineering Chemistry Research* 49, 9238-9247. DOI: 10.1021/ie901171b

Kuo, C. Y., Wu, C. H., and Chen, M. J. (2015). "Adsorption of lead ions from aqueous solutions by citric acid-modified celluloses," *Desalination and Water Treatment* 55, 1264-1270. DOI: 10.1080/19443994.2014.926460

Kurnik, K., Treder, K., Skorupa-Kłaput, M., Tretyn, A., and Tyburski, J. (2015). "Removal of phenol from synthetic and industrial wastewater by potato pulp peroxidases," *Water, Air, and Soil Pollution* 226, article 254. DOI: 10.1007/s11270-015-2517-0

Kuśmierek, K., Świątkowski, A., and Dąbek, L. (2017). "Removal of 2,4,6-trichlorophenol from aqueous solutions using agricultural waste as low-cost adsorbents," *Environment Protection Engineering* 43, 149-163. DOI: 10.5277/epel70412

Langmuir, I. (1917). "The constitution and fundamental properties of solids and liquids. II. Liquids," *Journal of the American Chemical Society* 39(9), 1848-1906. DOI: 10.1021/ja02254a006

Li, B., Akram, M., Al-Zuhair, S., Elnajjar, E., and Muhammad, T. M. (2020). "Subcritical water extraction of phenolics, antioxidants and dietary fibres from waste date pits," *Journal of Environmental Chemical Engineering* 8, article 104490. DOI: 10.1016/j.jece.2020.104490

Li, X., Wei, Y., Xu, J., Xu, N., and He, Y. (2018). "Quantitative visualization of lignocellulose components in transverse sections of moso bamboo based on ftir macro- and micro-spectroscopy coupled with chemometrics," *Biotechnology for Biofuels* 11, 1-16. DOI: 10.1186/s13068-018-1251-4

Nasser, R. A., Salem, M. Z. M., Hiziroglu, S., Al-Mefarrej, H. A., Mohareb, A. S., Alam, M., and Aref, I. M. (2016). "Chemical analysis of different parts of date palm (*Phoenix dactylifera* L.) using ultimate, proximate and thermo-gravimetric techniques for energy production," *Energies* 9(5), article 374. DOI: 10.3390/en9050374

Nazal, M. K., Gijjapu, D., and Abuzaid, N. (2021). "Study on adsorption performance of 2,4,6-trichlorophenol from aqueous solution onto biochar derived from macroalgae as an efficient adsorbent," *Separation Science and Technology (Philadelphia)* 56, 2183-2193. DOI: 10.1080/01496395.2020.1815778

Nourani, A., and Pegna, F. G. (2022). "A review on the mechanization of date palm cultivation," *Bulletin of the Transilvania University of Brasov, Series II: Forestry, Wood Industry, Agricultural Food Engineering* 15-64, 57-78. DOI: 10.31926/but.fwiafe.2022.15.64.1.5

Okasha, A. Y., and Ibrahim, H. G. (2010). "Phenol removal from aqueous systems by sorption of using some local waste materials," *Electronic Journal of Environmental, Agricultural and Food Chemistry* 9, 796-807.

Parthasarathy, P., Fernandez, A., Singh, D. K., Al-Ansari, T., Mackey, H. R., Rodriguez, R., Mazza, G., Tirkey, J. V., and McKay, G. (2022). "Thermogravimetric analysis of camel dung, date stone, and their blend for pyrolytic, kinetic, and thermodynamic studies," *Cleaner Chemical Engineering* 4(December), article 100072. DOI: 10.1016/j.clce.2022.100072

Pathania, D., Sharma, A., and Siddiqi, Z. M. (2016). "Removal of congo red dye from aqueous system using *Phoenix dactylifera* seeds," *Journal of Molecular Liquids* 219, 359-367. DOI: 10.1016/j.molliq.2016.03.020

Priyanka, O., Sudesh, R., and Kunwar, S. (2014). "Modified coconut fiber used as adsorbent for the removal of 2-chlorophenol and 2,4 ,6-trichlorophenol from aqueous solution," *South African Journal of Chemical Engineering* 19, 1-21.

Rezma, S., Assaker, I. Ben, litaiem, Y., Chtourou, R., Hafiane, A., and Deleuze, H. (2019). "Microporous activated carbon electrode derived from date stone without use of binder for capacitive deionization application," *Materials Research Bulletin* 111,

222-229. DOI: 10.1016/j.materresbull.2018.11.030

Santos Rocha, J., Dukheri, I. El, and Impiglia, A. (2018). "Date palm value chain development in the Arab countries: Key constraints and opportunities," in: *Sixth International Date Palm Conference*, pp. 1-18.

Sen, T. K. (2023). "Agricultural solid wastes based adsorbent materials in the remediation of heavy metal ions from water and wastewater by adsorption: A review," *Molecules* 28(14), article 5575. DOI: 10.3390/molecules28145575

Shafiq, M., Alazba, A. A., and Amin, M. T. (2018). "Removal of heavy metals from wastewater using date palm as a biosorbent: A comparative review," *Sains Malaysiana* 47, 35-49. DOI: 10.17576/jsm-2018-4701-05

Shaikh, H. M., Anis, A., Poulose, A. M., Al-Zahrani, S. M., Madhar, N. A., Alhamidi, A., and Alam, M. A. (2021). "Isolation and characterization of alpha and nanocrystalline cellulose from date palm (*Phoenix dactylifera* L.) trunk mesh," *Polymers* 13(11), article 1893. DOI: 10.3390/polym13111893

Siva Kumar, N., Asif, M., Poulose, A. M., Al-Ghurabi, E.H., Alhamedi, S. S., and Koduru, J. R. (2023). "Preparation, characterization, and chemically modified date palm fiber waste biomass for enhanced phenol removal from an aqueous environment," *Materials* 16(11), article 4057. DOI: 10.3390/ma16114057

Siva Kumar, N., Subba Reddy, A., Boddu, V. M., and Krishnaiah, A. (2009). "Development of chitosan-alginate based biosorbent for the removal of p-chlorophenol from aqueous medium," *Toxicological and Environmental Chemistry* 91, 1035-1054. DOI: 10.1080/02772240802541338

Siva Kumar, N., Woo, H. S., and Min, K. (2012a). "Equilibrium and kinetic studies on biosorption of 2,4,6-trichlorophenol from aqueous solutions by *Acacia leucocephala* bark," *Colloids and Surfaces B: Biointerfaces* 94, 125-132. DOI: 10.1016/j.colsurfb.2012.01.048

Soltani Goharrizi, R., Taghavi, L., Sarrafi, A., Karbasi, A., and Moradi Dehaghi, S. (2019). "Kinetic and isotherm study of 2,4,6-trichlorophenol's fast adsorption from aqueous solutions by synthesized magnetite-bentonite nanocomposite," *Journal of Water Chemistry and Technology* 41, 347-356. DOI: 10.3103/s1063455x1906002x

Thamilarasi, M. J. V., Anilkumar, P., Theivarasu, C., and Sureshkumar, M. V. (2018). "Removal of vanadium from wastewater using surface-modified lignocellulosic material," *Environmental Science and Pollution Research* 25, 26182-26191. DOI: 10.1007/s11356-018-2675-x

US EPA: Activated Carbon Adsorption of Trace Organic Compounds, http://nepis.epa.gov/Exe/ZyNET.exe/9100PI63.TXT?ZyActionD=ZyDocument&Client=EPA&Index=1976+Thru+1980&Docs=&Query=&Time=&EndTime=&SearchMethod=1&TocRestrict=n&Toc=&TocEntry=&QField=&QFieldYear=&QFieldMonth=&QFieldDay=&IntQFieldOp=0&ExtQFieldOp=0&XmlQuery=&, (1977)

Villegas, L. G. C., Mashhadi, N., Chen, M., Mukherjee, D., Taylor, K. E., and Biswas, N. (2016). "A short review of techniques for phenol removal from wastewater," *Current Pollution Reports* 2, 157-167. DOI: 10.1007/s40726-016-0035-3

Wang, P., Bian, X. F., and Li, Y. X. (2012). "Catalytic oxidation of phenol in wastewater – A new application of the amorphous Fe 78Si 9B 13 alloy," *Chinese Science Bulletin* 57, 33-40. DOI: 10.1007/s11434-011-4876-2

Wang, P., Ma, Q., Hu, D., and Wang, L. (2016). "Adsorption of methylene blue by a low-cost biosorbent: Citric acid modified peanut shell," *Desalination and Water Treatment* 57, 10261-10269. DOI: 10.1080/19443994.2015.1033651

Xu, Y., Liu, Y., Liu, S., Tan, X., Zeng, G., Zeng, W., Ding, Y., Cao, W., and Zheng, B. (2016). "Enhanced adsorption of methylene blue by citric acid modification of biochar derived from water hyacinth (*Eichornia crassipes*)," *Environmental Science and Pollution Research* 23, 23606-23618. DOI: 10.1007/s11356-016-7572-6

Yang, Z., Peng, H., Wang, W., and Liu, T. (2010). "Crystallization behavior of poly(ε-caprolactone)/layered double hydroxide nanocomposites," *Journal of Applied Polymer Science* 116, 2658-2667. DOI: 10.1002/app

Zada, A., Khan, M., Khan, M.A., Khan, Q., Habibi-Yangjeh, A., Dang, A., and Maqbool, M. (2021). "Review on the hazardous applications and photodegradation mechanisms of chlorophenols over different photocatalysts," *Environmental Research* 195, article 110742. DOI: 10.1016/j.envres.2021.110742

Zhou, L. C., Meng, X. G., Fu, J. W., Yang, Y. C., Yang, P., and Mi, C. (2014). "Highly efficient adsorption of chlorophenols onto chemically modified chitosan," *Applied Surface Science* 292, 735-741. DOI: 10.1016/j.apsusc.2013.12.041

Article submitted: January 29, 2024; Peer review completed: March 23, 2024; Revised version received and accepted: April 6, 2024; Published: April 17, 2024.
DOI: 10.15376/biores.19.2.3543-3570

# APPENDIX

## Materials and Methods

## Estimation of Best-Fitting Kinetic and Isotherm Studies Model Analysis

*Normalized standard deviation*

The normalized standard deviation was used to evaluate the validity of kinetic and equilibrium isotherm models:

$$\Delta q(\%) = 100 \times \sqrt{\sum_{i=1}^{N} \frac{\left[\left(q_{i,exp} - q_{i,cal}\right)/q_{i,exp}\right]^2}{(N-1)}} \quad (4)$$

where $q_i$, exp, and $q_i$, cal are time-dependent investigation data and the corresponding model predictions, respectively, whereas N represents the number of data points.

*Chi-Square Test ($\chi^2$)*

The chi-square analysis was performed to compare the agreement between the investigational data and the prediction models of kinetic and equilibrium isotherm. This is defined as [30],

$$\chi^2 = \sum_{i=1}^{N} \frac{\left(q_e - q_{e,model}\right)^2}{q_{e,model}} \quad (5)$$

where $q_e$ and $q_e$, model (mg/g) are the adsorbed amount of 2,4,6-TCP contaminant achieved experimentally and predicted by the relevant model, respectively.

## Characterization of Materials

*Particle size analysis*

The Laser Diffraction Particle Size Analyzer (SALD-2300, Shimadzu, Kyoto, Japan) determined particle size by analyzing the distribution pattern of scattered light from the sample particle surface.

*CHNS/O analyzer*

The date palm stone biomass samples were subjected to elemental analysis for carbon (C), hydrogen (H), and nitrogen (N) using a PerkinElmer 2400 CHNS/O series II analyzer (Norwalk, Connecticut, USA). The analyzer was operated in CHN mode. For each measurement, 2mg of the sample was used, and each measurement was conducted twice to ensure accuracy. The values reported are the average of the two measurements.

*Fourier transform infrared spectroscopy (FTIR)*

The surface functional groups of the adsorbent were determined using Fourier transform infrared spectrophotometry (Shimadzu, IR-PRESTIGE-21) with a spectral range of 400-4000 $cm^{-1}$.

*BET (Brunauer, Emmett, and Teller) analysis*

The BET method was used to measure the specific surface area, pore volume, and average pore size, making it an important technique for studying materials.

*Scanning electron microscope (SEM)*

The SEM (JSM-6360A-JEOL, Tokyo, Japan) and Energy-Dispersive X-ray Spectroscopy (EDX) facility were used to analyze the morphological and elemental aspects of the sample. In order to improve the quality of the image and prevent charging, a gold coating was applied to the sample using an auto fine coater (JFC/1600) for a period of 40 seconds.

*Thermogravimetric analysis (TGA)*

TGA analysis was carried out using a Shimadzu thermal analyzer (Model: DTG-60H, Simultaneous DTA-TG). To begin, the platina pan was filled with approximately 10-15 mg of the sample. The samples were then heated from room temperature up to 600℃ at a rate of 10 ℃ per minute. The analysis was conducted under a nitrogen atmosphere with a flow rate of 100 $cm^3$/min, and the corresponding weight loss was recorded.

## Adsorption Kinetic Models

The mathematical expression of the PFO kinetic model is as follows:

$$log(q_e - q_t) = -\frac{k_1}{2.303}t + logq_e \quad (6)$$

where the rate constant $k_1$ (1/min) can be evaluated using the slope of time versus $log(q_e - q_t)$ plot.

The PSO kinetic model can be stated as,

$$\frac{t}{q_t} = \frac{1}{q_e}t + \frac{1}{k_2 q_e^2} \quad (7)$$

Plotting $t$ versus $t/q_t$ yields $1/q_e$ (g/mg) as the slope, while the PSO rate constant $k_2$ (g/mg min) can be evaluated from the plot intercept.

Elovich equation's linear form can be stated as,

$$q_t = \frac{1}{b}\ln t + \frac{\ln(ab)}{b} \quad (8)$$

The parameter '$a$' represents the initial adsorption rate, while the parameter '$b$' (g/mg) is associated with the degree of surface coverage and the activation energy of chemisorption. When plotting ln$t$ *vs*. $q_t$, the slope is equal to 1/$b$, and the intercept is ln($ab$)/$b$.

In order to determine the rate-controlling for the sorption process, the researchers utilized the Intraparticle Diffusion (Webber and Morris) model, which is expressed by Eq. (10).

$$q_t = k_{id}\sqrt{t} + C \quad (9)$$

where the $k_{id}$ is the slope (mg/g.$min^{1/2}$) of $\sqrt{t}$ versus qt plot while the y-intercept $C$ is the thickness of the boundary layer.

## Adsorption Isotherm Models

The Langmuir isotherm equation in general form can be expressed as,

$$\left(\frac{1}{q_e}\right) = \frac{1}{K_L q_m}\left(\frac{1}{C_e}\right) + \frac{1}{q_m} \quad (10)$$

The equation involves the Langmuir coefficient ($K_L$), monolayer sorption capacity ($q_m$), and equilibrium concentration of the solute in solution ($C_e$). By plotting $1/q_e$ versus $1/C_e$, both $q_m$ and $K_L$ can be determined.

The Freundlich isotherm model is used to describe the non-ideal adsorption behavior of sorbents. Freundlich isotherm model represented as,

$$q_e = K_F C_e^{1/n} \quad (11)$$

Here $K_F$ ((mg/g)(L/mg)$^{1/n}$) represents 'relative adsorption capacity' while the parameter ($1/n$) designates 'adsorption intensity'.

The linearized form of Equation (11) is:

$$\ln q_e = \left(\frac{1}{n}\right)\ln C_e + \ln K_F \quad (12)$$

At equilibrium, the amount adsorbed ($q_e$) of adsorbate (mg/g) depends on the concentration of the adsorbate ($C_e$) in the solution (mg/L), as well as the Freundlich constants $K_F$ and $n$, which relate to adsorption capacity and intensity of adsorption, respectively.
The Dubinin–Radushkevich isotherm can be written as,

$$q_e = q_s \exp\left(-B\varepsilon^2\right) \quad (13)$$

where the parameter $B$ represents the sorption energy and $q_s$ is the D-R monolayer capacity (mg/g). The Polanyi potential, represented by $\varepsilon$, is defined by the equation:

$$\varepsilon = RT \ln\left[1 + \frac{1}{C_e}\right] \quad (14)$$

Using the parameter '$B$' in Eq. (15), the mean free adsorption energy ($E$) per adsorbate molecule can be computed as follows,

$$E = \frac{1}{\sqrt{2B}} \quad (15)$$

A plot of $\ln(q_e)$ versus $\varepsilon^2$ will enable the evaluation of isotherm parameters $q_s$ and $E$.

## SUPPLEMENTARY FIGURES

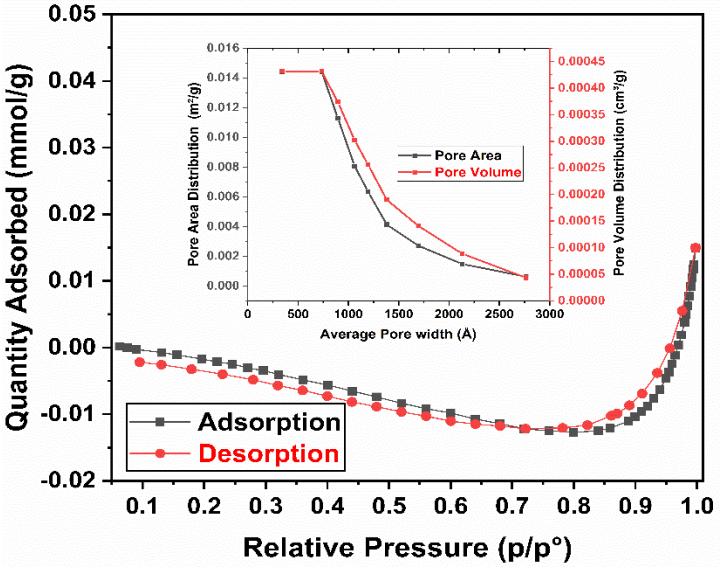


**Fig. S1.** $N_2$ adsorption–desorption isotherms and cumulative pore size and pore volume for raw date palm stone biomass

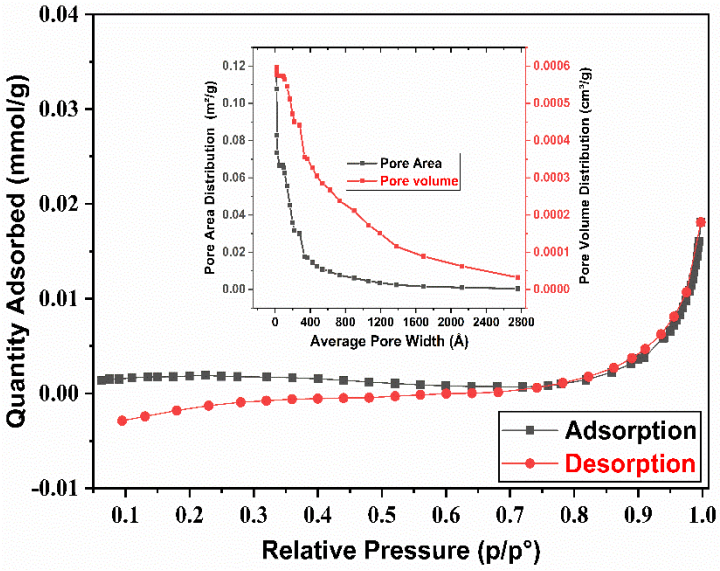


**Fig. S2.** $N_2$ adsorption–desorption isotherms and cumulative pore size and pore volume for 24 hrs ball-milled date palm stone biomass

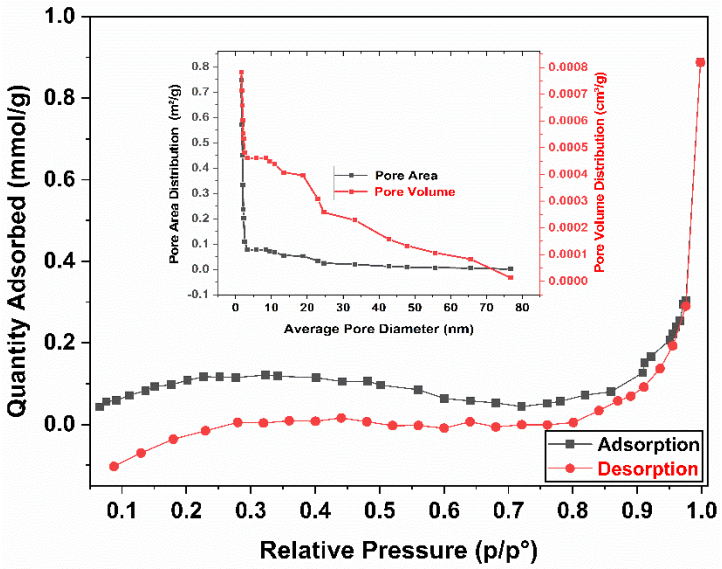


**Fig. S3.** $N_2$ adsorption-desorption isotherms and cumulative pore size and pore volume for 30 min Micro ball-milled date palm stone biomass (RDSB)

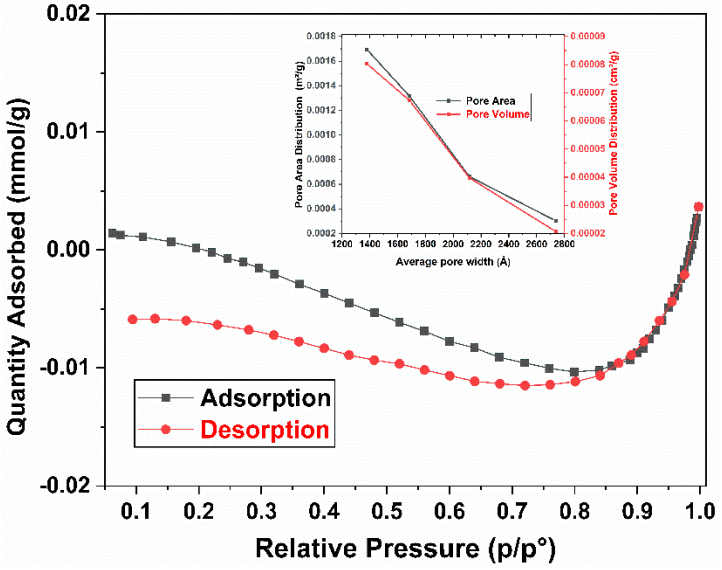


**Fig. S4**. $N_2$ adsorption–desorption isotherms and cumulative pore size and pore volume of CA-modified date palm stone biomass (CA–MDSB)

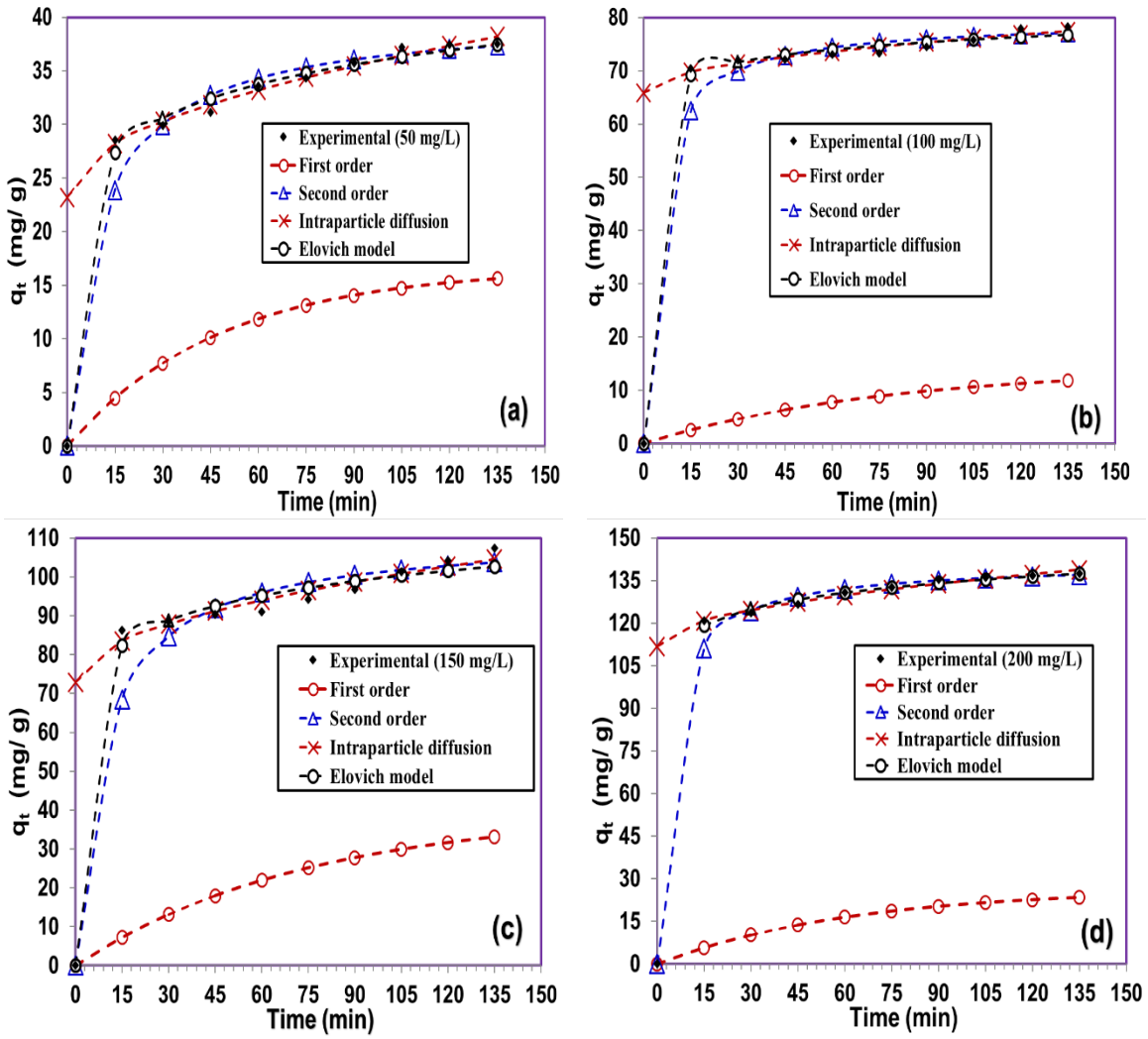


**Fig. S5(a-d).** RDSB biomass comparison results of experimental and calculated values obtained from the PFO, PSO, intraparticle diffusion and Elovich kinetic models

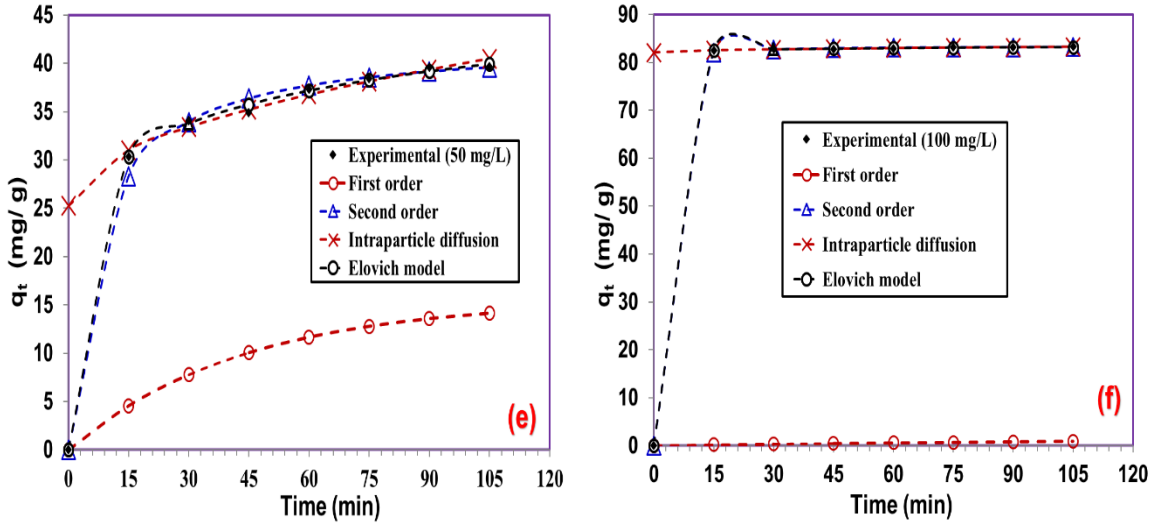

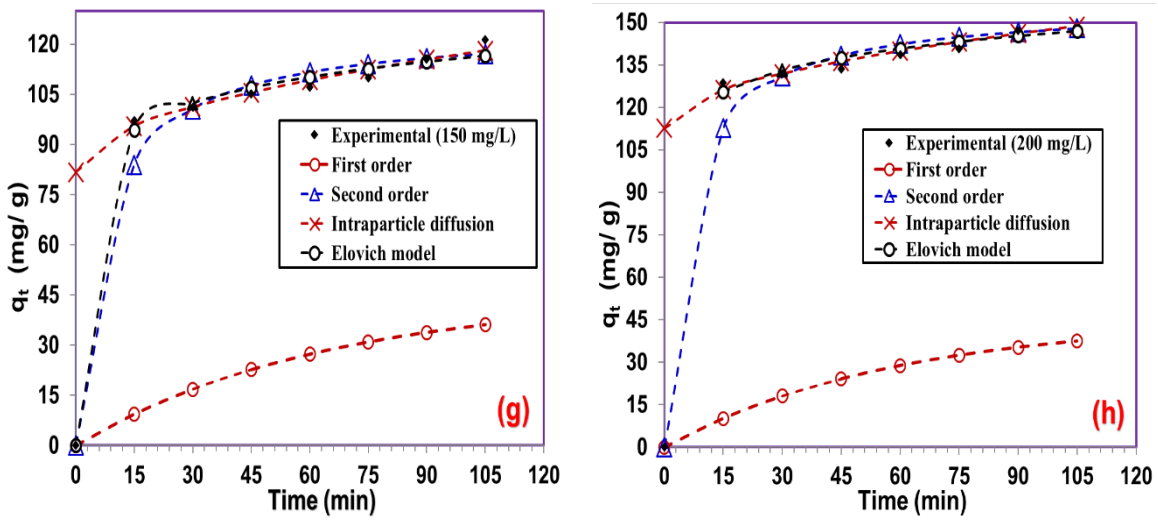


**Fig. S6(e-h).** CA-MDSB biomass **c**omparison results of experimental and calculated values obtained from the PFO, PSO, intraparticle diffusion and Elovich kinetic models

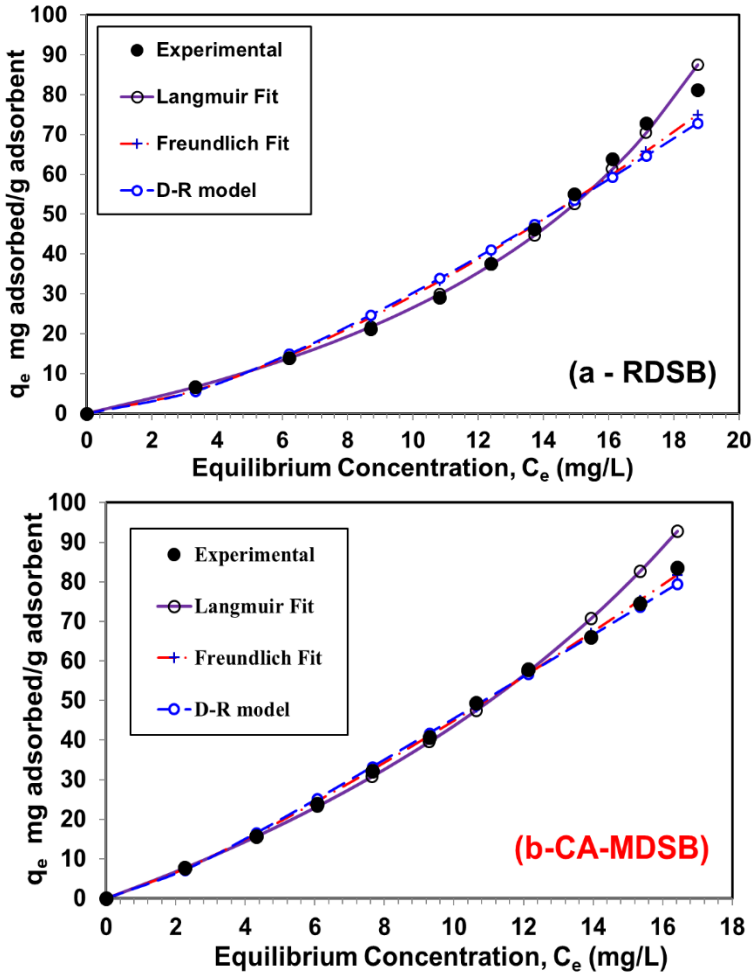


**Fig. S7(a-b).** Comparison of experimental and theoretical adsorption parameter values of (a) RDSB and (b) CA–MDSB adsorbents from the Langmuir, Freundlich, D-R isotherm models